Hydrogels assembled from ovotransferrin fibrils and xanthan gum as dihydromyricetin delivery vehicles

Journal:	*Food & Function*
Manuscript ID	FO-ART-11-2019-002564.R1
Article Type:	Paper
Date Submitted by the Author:	28-Dec-2019
Complete List of Authors:	Wei, Zihao; Rutgers University Chen, Yongsheng; Rutgers The State University of New Jersey Wijaya, Wahyu; Rutgers University Cheng, Yujia; Rutgers University Xiao, Jie; Rutgers The State University of New Jersey Huang, Qingrong; Rutgers University, Department of Food Science, , 65 Dudley Road, ,

SCHOLARONE™
Manuscripts

Hydrogels assembled from ovotransferrin fibrils and xanthan gum as dihydromyricetin delivery vehicles

Zihao Wei [a], Yongsheng Chen [a,b], Wahyu Wijaya [a,c], Yujia Cheng [a], Jie Xiao [d], Qingrong Huang [a,*]

[a] *Department of Food Science, Rutgers University, 65 Dudley Road, New Brunswick, New Jersey 08901, United States*

[b] *Department of Food Science and Engineering, Jinan University, Guangzhou 510632, China*

[c] *Enzyme and Protein Chemistry Group, Department of Bioengineering, Technical University of Denmark, Søltofts Plads, Building 224, 2800 Kgs. Lyngby, Denmark*

[d] *College of Food Science, South China Agricultural University, Guangzhou, 510642, China*

* To whom correspondence should be addressed. Tel: +1 (848) 932-5514. Fax: +1 (732) 932-6776. Email: qhuang@sebs.rutgers.edu

ABSTRACT:

The present study aimed to assemble protein fibril–polysaccharide hydrogels as nutraceutical delivery vehicles. Turbidity titrations confirmed that complexations between ovotransferrin (OVT) fibril and xanthan gum (XG) indeed existed, and electrostatic interaction was the major driving force of OVT fibril–XG complexation. After optimization of pH and acidifier, stable OVT fibril–XG hydrogel could be fabricated by adjusting pH to 4.0 with glucono delta-lactone. To better understand physicochemical properties of OVT fibril–XG gel, characterization of XG gel was also conducted. Scanning electron microscopy indicated that OVT fibril–XG gel had denser network than XG gel. Rheological measurements revealed that OVT fibril–XG gel had higher gel strength and viscosity than XG gel. OVT fibril–XG gel and XG gel could be applied as dihydromyricetin (DMY) delivery vehicles with a higher DMY loading (2 mg/mL). DMY release was investigated using *in vitro* gastrointestinal digestion model. All of DMY was released from OVT fibril–XG gel after gastrointestinal digestion, and only 41.7% of DMY was released from XG gel after gastrointestinal digestion, indicating that OVT fibril–XG gel was more efficient in DMY delivery. DMY was released via non-Fickian transport mechanism in both OVT fibril–XG gel and XG gel. The results in this study could provide new insight into assembly of protein fibril–polysaccharide hydrogels and rational design of hydrogels as nutraceutical delivery vehicles.

1. Introduction

Food protein fibrils are anisotropic food protein aggregates with linear structures, and food protein fibrils have been widely applied in assembly of food delivery systems due to excellent biocompatibility.[1–6] Although complexations between native proteins and polysaccharides have been extensively studied,[7–9] complexations between protein fibrils and polysaccharides have not attracted enough attention. During recent years, complexations between protein fibrils and polysaccharides have been confirmed,[10] and protein fibril–polysaccharide complexes have been applied to construct food-grade delivery vehicles such as emulsions.[11]

Hydrogel is a major class of nutraceutical delivery system with benefits such as pH-responsive delivery and controlled release.[12] Hydrogels assembled from proteins and polysaccharides under electrostatic associative conditions were first reported in 2006,[13,14] and protein–polysaccharide hydrogels have recently attracted increasing attention due to many advantages.[15,16] First, in comparison with protein hydrogels and polysaccharide hydrogels, gelation of protein–polysaccharide hydrogels often occurs at a lower polymer concentration.[17] Second, protein–polysaccharide hydrogels are fabricated without addition of harmful chemicals such as cross-linkers.[18] Third, protein–polysaccharide hydrogels may be easily degraded in gastrointestinal tract, which contributes to high release rate of nutraceuticals.[15] Fourth, protein–polysaccharide hydrogels can be fully made of food-grade biopolymers, which endows the hydrogel with outstanding biocompatibility.[16] To the best of our knowledge, protein–polysaccharide hydrogels are mainly assembled from native proteins and polysaccharides, and hydrogels assembled from protein fibrils and polysaccharides under electrostatic associative conditions have not been reported before. Since protein fibrils have

desirable prerequisites such as high aspect ratio, large contour length, random orientation, high stiffness and elasticity during gelation,[1,19] it is expected that protein fibrils may be more suitable for assembly of protein–polysaccharide hydrogels than native proteins. Protein fibril–polysaccharide hydrogels may possibly have unique physicochemical properties among all gels, and it is intriguing to investigate protein fibril–polysaccharide hydrogels systematically.

In our previous study, ovotransferrin (OVT) fibrils with excellent biocompatibility and digestibility can be assembled,[2, 20–23] so OVT fibril can be selected as protein fibril model to assemble protein fibril–polysaccharide hydrogels. Since xanthan gum (XG) is a common food additive with large-scale industrial production,[24] XG may be chosen as polysaccharide model to assemble protein fibril–polysaccharide hydrogels. In our preliminary experiments, it was found that XG could form transparent hydrogels at high polymer concentrations (≥ 30 mg/mL). Since comparison between protein–polysaccharide electrostatic hydrogels and polysaccharide hydrogels has recently aroused increasing interest,[14] it is intriguing to compare OVT fibril–XG hydrogels and XG hydrogels systematically. The acquired knowledge may help to better understand physicochemical properties of protein fibril–polysaccharide hydrogels.

Hydrogels have been widely applied as delivery vehicles for nutraceuticals and drugs due to several intriguing features.[12,15,25] For example, although many nutraceuticals such as curcumin have limited solubility in water at room temperature, hydrogels can load a significant amount of these nutraceuticals by trapping them within the gel compartments.[26] Dihydromyricetin (DMY) is the most abundant natural flavonoid in rattan tea, and DMY

possesses health benefits such as hepatoprotection, cardioprotection as well as neuroprotection.[27] However, bioefficacy of DMY has been severely limited due to low solubility of DMY at room temperature, and fabricating hydrogels with increasing DMY loading may be a feasible tool to improve bioefficacy of DMY. Thus, it is intriguing to apply OVT fibril–XG hydrogels as potential carriers for gastrointestinal delivery of DMY, and the relevant research may help to evaluate nutraceutical delivery performance of OVT fibril–XG hydrogels.

Accordingly, the objectives of this work were to fabricate OVT fibril–XG gels with OVT fibril and XG as building blocks under electrostatic associative conditions. Afterwards, gel characteristics such as syneresis, water holding capacity, microstructure and rheology were investigated. Finally, OVT fibril–XG gels were applied as DMY delivery vehicles, and gastrointestinal release of DMY was examined. In this study, XG gel was also investigated to better understand physicochemical properties of OVT fibril–XG gels. Hopefully, this work may provide new insights into fabrication and application of protein fibril–polysaccharide hydrogels.

2. Materials and methods

2.1. Materials

Ovotransferrin (OVT) with a purity above 88% and molecular weight around 76 kDa was purchased from Neova Technologies Inc. (Abbotsford, Canada). The manufacturer reported that iron content of the ovotransferrin was 1099 μg Fe/g. Xanthan gum (prehydrated Ticaxan rapid powder) was provided by TIC Gums (Belcamp, USA). Dihydromyricetin

(DMY) with a purity of 98% was obtained from JIAHERB Inc. (Pine Brook, USA). Glucono delta-lactone (GDL) was purchased from Acros Organics (Geel, Belgium). Other chemicals were of analytical grade and purchased from Sigma-Aldrich (St. Louis, USA) unless otherwise stated. Ultrapure water for all experiments was purified by a Milli-Q system (Burlington, USA).

2.2. Preparation of OVT fibrils

OVT fibrils were prepared as previously described with minor modifications.[4] OVT (50 mg/mL) was dissolved in pH-preset Milli-Q water (pH 2, 100 mM NaCl) under continuous stirring at 25 °C for 4 h, and sodium azide (0.02%, w/v) was added to restrain microbial growth. To obtain OVT fibrils, OVT solution in the sealed vials was heated at 90 °C and a stirring speed of 350 rpm for 26 h. The acquired OVT fibrils were dialyzed (molecular weight cutoff 15000 Da) against pH-preset water (pH 2) at 4 °C to eliminate NaCl in fibril dispersions. Afterwards, final concentration of OVT fibril dispersion was adjusted to 30 mg/mL with careful addition of pH-preset water (pH 2).

2.3. Interactions between OVT fibril and xanthan gum

2.3.1. Turbidimetric titration

Turbidimetric titration was applied to investigate interactions between OVT fibrils and xanthan gum (XG). Equal volumes of OVT fibril dispersion (0.8 mg/mL) and XG solution (0.4 mg/mL) were mixed homogeneously, and OVT fibril/XG mass ratio was 2:1. Before turbidimetric titration, pH of OVT fibril–XG mixture was adjusted to 9 with 0.2 M NaOH.

A Brinkmann PC910 colorimeter (Metrohm, Riverview, USA) with a 1-cm path length

optical probe and a 420-nm filter was employed to measure pH-dependent turbidity, and the colorimeter was calibrated to read 100% transmittance (T) with Milli-Q water.[28] Turbidity was defined as 100– T%, and turbidity titrations were carried out at 25 °C under continuous stirring. The titration was performed from high pH to low pH, and HCl solutions with concentration gradients (0.05–1 M) were used to adjust pH to minimize the dilution effect. To help clarify interactions between OVT fibril and XG, turbidity measurements of OVT fibril and XG were conducted as controls.

2.3.2. Zeta potential

To understand electrostatic interactions between OVT fibril and XG, zeta potential of OVT fibril, XG and OVT fibril–XG mixture (mass ratio $r = 2:1$) at biopolymer concentration of 1 mg/mL was measured with the aid of Zetasizer Nano-ZS90 instrument (Malvern Instruments, Worcestershire, UK).[29]

2.4. Hydrogel formation

2.4.1. Preparation of OVT fibril–XG gel

2.4.1.1. Successful formation of OVT fibril–XG gel

The pH of OVT fibrils and XG was first adjusted to 6.5. Afterwards, OVT fibril dispersion (30 mg/mL) and XG solution (30 mg/mL) were mixed homogeneously at volume ratio of 2:1, and total biopolymer concentration in the mixture was 30 mg/mL. GDL was slowly added into the mixture under constant stirring (100 rpm) to achieve homogeneous distribution, followed by aging (unstirred and undisturbed) at 25 °C for 24 h. The final pH of the mixture was 4.0. Vial inversion method was employed to examine successful formation

of hydrogel. The vials were inverted, and samples without flow for 24 h at 25 °C were regarded as stable hydrogels.

2.4.1.2. Impact of acidifier and final pH on OVT fibril–XG gel formation

Impact of acidifier and final pH on OVT fibril–XG gel formation was also investigated. In terms of acidifier, HCl was applied to adjust pH to 4.0 instead of GDL, and all other procedures were the same as described in 2.4.1.1. In terms of final pH, the final pH of the mixture was adjusted to 2.5 and 3.2 using GDL, and all other procedures were the same as described in 2.4.1.1.

2.4.2. Preparation of XG gel

To help understand physicochemical properties of OVT fibril–XG gel, XG gel was also prepared. XG (30 mg/mL) was dissolved in pH-adjusted water (pH 4.0) at 60 °C for 5 min, followed by sonication to remove trapped bubbles. Subsequently, XG was aged (unstirred and undisturbed) at 25 °C for 24 h, and vial inversion method was applied to examine successful formation of XG gel. Impact of biopolymer concentration on XG gel formation was also investigated. XG solution (10 mg/mL) was prepared by thermal dissolution, and all other procedures were the same as mentioned above.

2.5. Characterization of OVT fibril–XG gel and XG gel

2.5.1. Syneresis

To determine syneresis, OVT fibril–XG gel and XG gel in vials were stored upside down at 25 °C for 120 min, and the amount of expelled water was quantified.[30] Syneresis was

determined based on following equation:

$$\text{syneresis} = \frac{\text{weight of expelled water}}{\text{weight of gel sample}} \times 100 \qquad (1)$$

2.5.2. Water holding capacity

OVT fibril–XG gel and XG gel in centrifuge tubes were centrifuged at 1500 × g for 10 min, and the released water during centrifugation was weighed.[31] Water holding capacity was determined as follows:

$$\text{water holding capacity} = (1 - \frac{\text{weight of released water}}{\text{weight of gel sample}}) \times 100 \qquad (2)$$

2.5.3. Scanning electron microscopy (SEM)

The microstructures of OVT fibril–XG gel and XG gel were characterized by field emission scanning electron microscopy (FESEM, JEOL JSM-7900F, Japan). Around 50 μL of OVT fibril–XG gel and XG gel was deposited onto aluminum stubs, followed by sequential drying at 25 °C.[15] The gel samples were subsequently coated in a Quorum sputter coater (Quorum Technologies, East Sussex, UK) with a thin layer of gold, followed by SEM imaging.

2.5.4. Rheology

The rheological properties of XG gel and OVT fibril−XG gel were characterized at 25.0±0.1 °C employing a Discovery HR-2 rheometer (TA Instruments, New Castle, USA) with a parallel plate geometry (diameter 25 mm, gap 1 mm). The gel samples were deposited onto the rheometer plate, followed by 5 min setting time to allow thermal equilibrium. To

investigate the dynamic oscillation characteristics, dynamic frequency sweep test was carried out at a fixed strain amplitude of 0.2% (within the linear viscoelastic region), and storage modulus (G') as well as loss modulus (G'') of gel samples were recorded versus frequency. Steady-state flow measurements were also conducted, and apparent viscosity of gel samples as a function of shear rate was measured.

2.6. Preparation of DMY-loaded hydrogels

2.6.1. Preparation of DMY-loaded OVT fibril–XG gel

XG (30 mg/mL) and DMY (6 mg/mL) were dissolved in pH-adjusted water (pH 4.0) under constant stirring at 60 °C for 5 min, followed by pH adjustment to 6.5. XG–DMY mixture was mixed homogeneously with OVT fibril (30 mg/mL, pH 6.5) at volume ratio of 1:2. The final concentration of OVT fibril, XG and DMY was 20 mg/mL, 10 mg/mL and 2 mg/mL, respectively. Afterwards, GDL was slowly added into the mixture under constant stirring to achieve homogeneous distribution, and final pH of the mixture was 4.0. After aging (unstirred and undisturbed) at 25 °C for 24 h, stable OVT fibril–XG gel with a DMY loading of 2 mg/mL was acquired.

2.6.2. Preparation of DMY-loaded XG gel

XG (30 mg/mL) and DMY (2 mg/mL) were dissolved in pH-adjusted water (pH 4.0) under constant stirring at 60 °C for 5 min, followed by sonication to eliminate trapped bubbles. After aging without disturbance at 25 °C for 24 h, stable XG gel with a DMY loading of 2 mg/mL was obtained.

2.7. Gastrointestinal release of DMY from OVT fibril–XG gel and XG gel

Simulated gastric fluid was obtained by adding 0.2 g of NaCl and 0.16 g pepsin into 100 mL of pH-adjusted water (pH 1.2).[28] For the stage of simulated gastric digestion, 10 g of DMY-loaded gel samples (OVT fibril–XG gel and XG gel) were mixed with 30 mL of simulated gastric fluid, followed by incubation at 37.0±0.2 °C for 2 h. The gastric digestion was terminated through raising pH to 6.8 to inactivate pepsin.[3]

Simulated intestinal digestion followed gastric digestion, and simulated intestinal fluid was obtained by adding 10 mg/mL bile salt, 10 mM $CaCl_2$ and 9.5 mg/mL pancreatin into Tris-maleate buffer (pH 6.8). To initiate intestinal digestion, the gastric digesta were mixed with simulated intestinal fluid at volume ratio of 1:1. To mimic small intestinal conditions, the mixture was incubated at 37.0±0.2 °C for 2 h. An aliquot of mixture was withdrawn at proper time intervals during gastrointestinal digestion, and the amount of released DMY was determined using HPLC as described in 2.8.

2.8. High-performance liquid chromatography (HPLC) analysis of DMY

The amount of released DMY was determined employing an Agilent 1100 Series HPLC system (Agilent Technologies, Santa Clara, USA) with a Synergi™ 4 μm Hydro-RP 80 Å (Phenomenex, Torrance, USA) column (250×4.6 mm i.d.). The mobile phase consisted of (A) acetonitrile and (B) water, and gradient elution was conducted at a flow rate of 0.5 mL/min. The gradient elution program was set as follows: 0−8 min, A went from 10% to 25% linearly; 8−16 min, linear gradient from 25% to 40% A; 16−20 min, A went from 40% to 55% linearly; 20−25 min, linear gradient from 55% to 10% A. The detection wavelength was 292 nm, and DMY content was calculated based on a standard curve of DMY.

2.9. Statistical analysis

All experiments were conducted in triplicate, and data analysis was performed by OriginPro 2019 software. One-way analysis of variance (ANOVA) with Fisher LSD test was applied to determine statistical differences, and differences with $p < 0.05$ were considered to be significant.

3. Results and discussion

3.1. Complexation between OVT fibril and XG

In comparison with complexations between native proteins and polysaccharides,[9,31] complexations between protein fibrils and polysaccharides remain largely unknown. To the best of our knowledge, so far only two papers confirm complexations between protein fibrils and polysaccharides with experimental evidence, and both papers focus on β-lactoglobulin fibrils.[10,11] Since β-lactoglobulin fibrils differ significantly from some protein fibrils such as OVT fibrils in morphology,[2,10] complexations between polysaccharides and some protein fibrils may not occur easily. In our previous studies, it has been demonstrated that native OVT can form strong complexes with polysaccharides such as sugar beet pectin and gum arabic,[7,8] suggesting that OVT is a protein with strong ability to interact with polysaccharides. Based on these understandings, OVT fibril is applied as a model to investigate protein fibril−polysaccharide complexations.

Because turbidity is related to the amount and size of biopolymer particles, turbidity changes may be employed to analyze associative and segregative phase behaviors within biopolymer mixtures.[31] During recent years, turbidimetric titrations have been widely applied

to investigate complexations between native proteins and polysaccharides.[7,8,31] In this work, complexations between OVT fibril and XG were also investigated using turbidimetric titrations. To better understand complexations between OVT fibril and XG, turbidity of either OVT fibril or XG was studied as control. As shown in Fig. 1, XG had negligible turbidity during the entire pH range, and OVT fibril had a turbidity around 7.4 at most pHs, indicating that OVT fibril with an average contour length of 337 nm could generate turbidity.[4] When pH was close to isoelectric point (pH 7.1, as evidenced in Fig. 2) of OVT fibril, it was found that turbidity of OVT fibril slightly increased in the pH range of 6.7–7.6, implying slight aggregation of OVT fibril at pH 6.7–7.6. Fig. 1 also depicts turbidity titration curve of OVT fibril–XG mixture. When pH was above 7.1, turbidity of OVT fibril–XG mixture was almost the same as that of OVT fibril alone, suggesting that complexations between OVT fibril and XG did not occur at pHs above 7.1. The turbidity of OVT fibril–XG mixture increased slowly when pH shifted downwards from 7.1 to 5.3, and an abrupt increase of turbidity was observed in OVT fibril–XG mixture when pH decreased from 5.2 to 2.6. The rise of turbidity in OVT fibril–XG mixture indicated that OVT fibril could interact with XG, and OVT fibril–XG complexes could be obtained successfully. As pH decreased from 2.6 to 1.0, turbidity decreased dramatically, indicating that a large amount of OVT fibril–XG complexes were dissociated into non-interacted OVT fibril and XG. It was noteworthy that turbidity of OVT fibril–XG mixtures was still higher than a combination of turbidity from OVT fibril and XG at pH 1.0, indicating that weak complexations between OVT fibril and XG still existed at pH 1.0. In our previous studies, when pH decreased to around 2.0, it was found that complexes between native OVT and polysaccharides were fully dissociated with a turbidity of zero.[7,8]

Thus, the remaining turbidity of OVT fibril–XG mixtures indicated that OVT fibrils could interact with polysaccharides more strongly than native OVT, which could be explained as follows. Native OVT is spherical with size around 3–5 nm, and OVT fibril has linear structures with an average contour length of 337 nm.[4] The larger size and linear shape of OVT fibril may facilitate stronger entanglements with polysaccharides, which may lead to remaining OVT fibril–polysaccharide complexes at very low pH.

It is speculated that complexations between OVT fibril and XG are mainly caused by electrostatic attractions, so zeta potential was investigated to confirm the speculation. As shown in Fig. 2, zeta potential of OVT fibril increased with the decrease of pH due to protonation of amine groups as well as deprotonation of carboxyl groups, and isoelectric point of OVT fibril was 7.1. As pH decreased from 9 to 2, zeta potential of XG increased from -64.3 ± 3.5 mV to -17.6 ± 2.1 mV. XG still carried sufficient negative charges at pH 2, which was in consistence with a previous study.[32] As discussed earlier, complexations between OVT fibril and XG were initiated at pH 7.1 (close to isoelectric point of OVT fibril), and this phenomenon could be explained by theory of electrostatic interactions between OVT fibril and XG. Specifically, both OVT fibril and XG carried negative charges above pH 7.1, and the electrostatic repulsions between them could prevent their complexation. When pH decreased to below 7.1, OVT fibril carried positive charges, and electrostatic attractions between OVT fibril and XG could contribute to their complexations. Fig. 2 shows that zeta potential of OVT fibril–XG mixture increased as pH decreased, and zeta potential of OVT fibril–XG mixture approached zero at pH 2.5, indicating that complete charge neutralization occurred at pH 2.5. It was noteworthy that the turbidity of OVT fibril–XG mixture reached

the maximal value at pH 2.5, suggesting that complete charge neutralization contributed to the maximal complexations between OVT fibril and XG. Based on the results of turbidity titration and zeta potential, it could be concluded that complexations between OVT fibrils and XG indeed existed, and the major driving force of OVT fibril–XG complexation was electrostatic attraction.

3.2. Fabrication of stable hydrogels

Protein gels are promising delivery platforms for nutraceuticals, and protein gels have attracted increasing attention in food science.[33,34] To fabricate protein gels, proteins are often unfolded through physical and chemical means, followed by aggregation of denatured molecules and formation of continuous ordered network.[35] Since OVT fibril was obtained after protein unfolding and aggregation of denatured molecules,[2] it was intriguing to find whether OVT fibril alone could form stable hydrogels. As shown in Fig. 3, OVT fibrils flowed to the bottom of vial during vial inversion test, indicating that stable hydrogels could not be constructed by OVT fibrils alone. Since electrostatic protein–polysaccharide complexations helped to construct hydrogels,[14] it was expected that electrostatic complexations between OVT fibrils and polysaccharides might contribute to formation of stable hydrogel, which could broaden application of OVT fibrils in nutraceutical delivery systems. Since xanthan gum (XG) had synergistic gelation with many biopolymers,[17,36] XG could be applied to construct hydrogels with OVT fibrils. To better understand gelling property of OVT fibril–XG complexes, gelling behavior of XG was also investigated. As shown in Fig. 4, XG at 10 mg/mL did not form stable hydrogel, but XG at 30 mg/mL could form transparent hydrogel. Considering that gelling ability of OVT fibril–XG complexes

should not be interfered with that of XG during preparation of OVT fibril–XG hydrogel, XG at a final concentration of 10 mg/mL was applied to fabricate stable hydrogels with OVT fibrils.

To fabricate OVT fibril–XG hydrogel through electrostatic interactions, proper pHs should be selected to ensure a sufficient degree of electrostatic interactions between OVT fibril and XG. As shown in Fig. 1, considering that complexes started to dissociate below pH 2.5, strong complexations between OVT fibril and XG existed in the pH range of 2.5–4.0. Therefore, fabrication of stable OVT fibril–XG hydrogel was mainly conducted at 2.5–4.0. As shown in Fig. S1 and Fig. S2 (see Supplementary Information), hydrogels assembled from OVT fibril (20 mg/mL) and XG (10 mg/mL) at pH 2.5 and pH 3.2 flowed during vial inversion test, suggesting that stable hydrogels could not be fabricated at pH 2.5 and pH 3.2. The phenomenon can be explained as follows. Gelation and phase separation exist simultaneously in the system, and they may compete with each other.[13] At pH 2.5 and pH 3.2, as indicated in Fig. 1, complex coacervation of OVT fibril and XG occurs, which results in significant phase separation. The strong phase separation inhibits gelation via competition mechanism, which leads to formation of unstable gel at pH 2.5 and pH 3.2. Fig. 5 shows that hydrogels assembled from OVT fibril (20 mg/mL) and XG (10 mg/mL) at pH 4.0 could withstand vial inversion test for 24 h, indicating that stable hydrogel could be fabricated at pH 4.0. As mentioned earlier, either OVT fibril (20 mg/mL) or XG (10 mg/mL) could not form stable hydrogels, so it could be concluded that there was a synergistic gelation of OVT fibril with XG via electrostatic complexation mechanism.

Since acidifier could exert great impact on gel formation, influence of acidifier on

formation of OVT fibril–XG hydrogel was also studied. Fig. 6 shows visual appearance of OVT fibril–XG hydrogel fabricated with the addition of HCl. It was obvious that the hydrogel was not homogeneous, and a lot of water was not trapped, which could be explained as follows. During our experiments, it was observed that acidification of OVT fibril–XG system using HCl resulted in significant precipitation, and the inhomogeneous distribution of biopolymers could hinder formation of stable hydrogel. When compared with HCl, addition of glucono delta-lactone (GDL) induced slow acidification of OVT fibril–XG system, and gel networks could arrange in three-dimensional networks without obvious precipitation. Considering that stable OVT fibril–XG hydrogels could be fabricated with the addition of glucono delta-lactone (GDL), it could be concluded that GDL was more suitable than HCl in fabricating protein fibril–polysaccharide hydrogels.

3.3. Characterization of OVT fibril–XG gel

After successful assembly of OVT fibril–XG gel, it was necessary to characterize OVT fibril–XG gel systematically before its application. As mentioned earlier in Fig. 4b, transparent XG gel could be assembled at XG concentration of 30 mg/mL. Thus, it was interesting to compare turbid OVT fibril–XG gel with transparent XG gel systematically, which facilitated deeper understandings into physicochemical properties of OVT fibril–XG gel. For rational comparison, the total biopolymer concentration of both OVT fibril–XG gel and XG gel was fixed at 30 mg/mL.

Gel syneresis is a process that a hydrogel undergoes macroscopic contraction, which results in expelled water from the hydrogel network.[37] Since hydrogel integrity is important

for many applications, it is necessary to investigate gel syneresis. As shown in Table 1, there was no syneresis for both OVT fibril–XG gel and XG gel, indicating that these gels kept integral without water expulsion. It was interesting to compare gel syneresis in this study with syneresis of other biopolymer hydrogels. In a previous study, agar hydrogel exhibited significant syneresis, and deformation of gel network could grow with increasing syneresis.[38] This phenomenon indicated that agar hydrogel was not as integral as OVT fibril–XG gel and XG gel.

The capacity of holding water was an important property of hydrogels, so water holding capacity of OVT fibril–XG gel and XG gel was investigated under centrifugal force.[30,39] Table 1 shows that water holding capacities of OVT fibril–XG gel and XG gel were 95.8% and 100.0%, respectively. The slightly lower water holding capacity of OVT fibril–XG gel can be explained as follows. First, the hydrophilic structures are critical to water holding of hydrogels, and more hydrophilic structures facilitate holding a larger amount of water in three-dimensional crosslinked networks.[40] Since OVT fibril is less hydrophilic than XG, it is reasonable to deduce that water holding capacity of OVT fibril–XG gel is lower than that of XG gel. Second, the location of OVT fibril and XG in OVT fibril–XG gel may change slightly during centrifugation, which possibly leads to alteration in electrostatic interactions between OVT fibril and XG. Since OVT fibril–XG gel is stabilized by electrostatic OVT fibril–XG interactions, the disruption of electrostatic interactions may be detrimental to structures of OVT fibril–XG gel, which results in weaker ability to retain water.

Because OVT fibril–XG gel and XG gel had significantly different compositions and

visual appearance, it was expected that OVT fibril–XG gel and XG gel could have different microstructures. SEM imaging was carried out to gain an insight into morphology of OVT fibril–XG gel and XG gel. As shown in Fig. 7a, XG gel had highly porous and interconnected structures. Fig. 7b shows that OVT fibril–XG gel had filamentous morphology with denser network. It was observed that pores also existed in OVT fibril–XG gel, and pore size of OVT fibril–XG gel was smaller than that of XG gel, which could be ascribed to an increase of crosslinking density in OVT fibril–XG gel. The denser interpolymeric network of OVT fibril–XG gel compared to XG gel was in agreement with our previous study on the acid-induced gelation of whey protein isolate and low-methoxyl pectin, in which the protein strengthened the jamming of the pectin networks.[16]

Rheological property was critical to physicochemical stability, processing and application of hydrogels, so rheological behavior of OVT fibril–XG gel and XG gel was investigated. As shown in Fig. 8a, storage modulus was significantly higher than loss modulus for both gels, indicating strong gel-like structures. It was also observed that storage modulus of OVT fibril–XG gel was higher than that of XG gel, suggesting that OVT fibril–XG gel had higher gel strength than XG gel. Fig. 8b depicts that both OVT fibril–XG gel and XG gel exhibited shear-thinning behaviors, which might be ascribed to disruption of crosslinked gel networks at a high shear rate and following rearrangement of three-dimensional networks in the flow direction. Fig. 8b also shows that viscosity of OVT fibril–XG gel was significantly higher than that of XG gel, It was summarized that OVT fibril–XG gel had higher gel strength and viscosity than XG gel, which could be explained as follows. As shown earlier in Fig. 7, OVT fibril–XG gel had denser networks than XG gel,

and the denser network could lead to more compact trapping network and higher resistance against gradual deformation by shear stress, which contributed to higher gel strength and viscosity.

3.4. Hydrogels as DMY delivery vehicles

Oil-in-water emulsions have been widely applied to deliver nutraceuticals in food science,[41–43] but ingestion of large amounts of oil may lead to health problems such as obesity and cardiovascular disease. Hydrogels are better delivery vehicles while taking health issues into account, and it is interesting to investigate nutraceutical delivery performance of OVT fibril–XG gel and XG gel. Dihydromyricetin (DMY) could be selected as a nutraceutical model to investigate nutraceutical delivery performance of hydrogels, which could be explained as follows. As shown in Fig. 9a, DMY could not be dissolved in water at room temperature, and only DMY suspension with existence of precipitation was obtained at room temperature, which hindered widespread application of DMY. Fig. 9b shows that heating was a feasible means to solubilize DMY. However, as shown in Fig. 9c, a large amount of heated DMY precipitated after storage at 25 °C for 6 h, indicating that heating could not fully solve poor solubility and dispersibility of DMY in water. Thus, delivery of DMY was in urgent need of suitable delivery vehicles, and assembly of DMY-loaded hydrogel could be a feasible solution to improve DMY loading.

DMY (dissolved under heating treatment) with a final concentration of 2 mg/mL was loaded into hydrogels, and visual appearance of DMY-loaded hydrogels was shown in Fig. S3 and Fig. S4 (see Supplementary Information). As depicted in Fig. S3, DMY-loaded XG

gel was homogeneous with transparent appearance, and no precipitation was observed at room temperature, suggesting that XG gel could load DMY perfectly by trapping it within crosslinked networks. Fig. S4 shows that DMY-loaded OVT fibril–XG gel was homogeneous with turbid appearance, which was similar to visual appearance of OVT fibril–XG gel with no encapsulated DMY in Fig. 5. Stable and homogeneous DMY-loaded OVT fibril–XG gel indicated that OVT fibril–XG gel could encapsulate DMY effectively.

Release of nutraceuticals from hydrogels could have characteristics such as pH-responsivness and controlled release,[12,34] and it was interesting to understand release profiles of DMY from OVT fibril–XG gel and XG gel. DMY release from OVT fibril–XG gel and XG gel was investigated using *in vitro* gastrointestinal digestion model, and release profiles of DMY were shown in Fig. 10. As depicted in Fig. 10, 23.2 percent of DMY was released from XG gel during gastric digestion, and 96.5 percent of DMY was released from OVT fibril–XG gel during gastric digestion, indicating that most of encapsulated DMY was released from OVT fibril–XG gel. The higher release rate of DMY from OVT fibril–XG gel during gastric digestion can be explained as follows. First, OVT fibril–XG gel is fabricated and stabilized by electrostatic interactions at pH 4.0, and pH 1.2 of simulated gastric fluid can disrupt electrostatic interactions within OVT fibril–XG gel, which contributes to collapse of crosslinked networks. Most of DMY can be released during degradation of OVT fibril–XG gel. Second, a significant amount of OVT fibrils may be digested by pepsin during gastric digestion.[20,44] The destruction of OVT fibrils may result in breakdown of OVT fibril–XG gel, which contributes to rapid release of DMY. Third, since XG is not digested by pepsin and XG gel is not very sensitive to pH changes, XG gel is relatively stable in comparison with

OVT fibril–XG gel. Although swelling of XG gel can contribute to release of DMY, the release rate from XG gel is relatively slow without contribution of massive gel breakdown. As shown in Fig. 10, after a combination of gastric and intestinal digestion, the release rates of DMY from XG gel and OVT fibril–XG gel were 41.7% and 100.0%, respectively, indicating that all of encapsulated DMY in OVT fibril–XG gel was released during gastrointestinal digestion. It was also found that DMY release rate of XG gel (18.5%) was higher than that of OVT fibril–XG gel (3.5%) during intestinal digestion.

It was interesting to explore the mechanism of DMY release from OVT fibril–XG gel and XG gel. Based on a previous study,[34] the mechanism of DMY release from the hydrogels could be determined by Korsmeye–Peppas semi-empirical equation:

$$M_t/M_\infty = kt^n \tag{3}$$

where M_t was the amount of DMY released after time t, M_∞ was the amount of DMY released at infinite time, k was a constant and n was the diffusional exponent (dimensionless). The diffusional exponent n reflected release mechanism of nutraceuticals: $n \leq 0.43$ indicated Fickian diffusion, $0.43 < n < 0.89$ indicated non-Fickian transport, and $n \geq 0.89$ indicated case Ⅱ transport.[34] The high correlation coefficient R^2 (>0.94) indicated that Korsmeye–Peppas semi-empirical equation fitted DMY release data adequately. DMY release from OVT fibril–XG gel had n value of 0.48, indicating that DMY was released from OVT fibril–XG gel via non-Fickian transport mechanism. The non-Fickian release implied that release of DMY from OVT fibril–XG gel did not obey Fickian diffusion theories, and diffusing DMY could cause deformation which induced viscoelastic stress that interacted with Brownian

motion of the fluid molecules.[45,46] It was found that DMY release from XG gel also followed non-Fickian transport mechanism ($n = 0.67$).

After systematic analysis of DMY release profiles, it is necessary to compare nutraceutical delivery performance of OVT fibril–XG gel and XG gel. First, most of nutraceuticals are released from OVT fibril–XG gel during gastric digestion, indicating that OVT fibril–XG gel can be applied as stomach-specific nutraceutical delivery vehicles. Since only a very small part of nutraceuticals are released from OVT fibril–XG gel during intestinal digestion, OVT fibril–XG gel may not function well for intestinal delivery of nutraceuticals. XG gel may be a better option to achieve intestinal delivery of nutraceuticals. Second, if higher nutraceutical release rate instead of target delivery is the goal, OVT fibril–XG gel is a better option in comparison with XG gel. That's because more nutraceuticals may be released from OVT fibril–XG gel, which contributes to higher bioefficacy of nutraceuticals. The acquired knowledge may facilitate selection of proper hydrogels as nutraceutical delivery systems.

4. Conclusion

In summary, complexations between OVT fibril and XG indeed existed, and electrostatic interaction was the major driving force of OVT fibril–XG complexation. Stable hydrogels could be fabricated using OVT fibril and XG at pH 4.0 and mass ratio of 2:1. OVT fibril–XG gel had higher gel strength and viscosity than XG gel. OVT fibril–XG gel and XG gel could be developed as DMY delivery vehicles with improved DMY loading. In terms of gastrointestinal release, 96.5% of DMY was released from OVT fibril–XG gel during gastric

digestion, and all of DMY was released from OVT fibril–XG gel after gastrointestinal digestion. Only 41.7% of DMY was released from XG gel after gastrointestinal digestion, and DMY release rate from XG gel during gastric and intestinal digestion was 23.2% and 18.5%, respectively. DMY was released via non-Fickian transport mechanism in both OVT fibril–XG gel and XG gel. To the best of our knowledge, this should be the first study about preparation and application of food-grade protein fibril–polysaccharide hydrogels. The knowledge gained from this work could facilitate assembly of protein fibril–polysaccharide hydrogel and rational design of hydrogels as nutraceutical delivery vehicles.

Declaration of interests

There are no conflicts of interest to declare.

Acknowledgements

References

1. Y. Cao and R. Mezzenga, Food protein amyloid fibrils: Origin, structure, formation, characterization, applications and health implications, *Adv. Colloid Interfac.*, 2019, **269**, 334–356.

2. Z. Wei and Q. Huang, Assembly of iron-bound ovotransferrin amyloid fibrils, *Food Hydrocolloids*, 2019, **89**, 579–589.

3. Z. Wei and Q. Huang, Developing organogel-based Pickering emulsions with improved freeze-thaw stability and hesperidin bioaccessibility, *Food Hydrocolloids*, 2019, **93**, 68–77.

4. Z. Wei, J. Cheng and Q. Huang, Food-grade Pickering emulsions stabilized by ovotransferrin fibrils, *Food Hydrocolloids*, 2019, **94**, 592–602.

5. Z. Wei and Q. Huang, Modification of ovotransferrin by Maillard reaction: Consequences for structure, fibrillation and emulsifying property of fibrils, *Food Hydrocolloids*, 2019, **97**, 105186.

6. Z. Wei, J. Zhu, Y. Cheng and Q. Huang, Ovotransferrin fibril–stabilized Pickering emulsions improve protection and bioaccessibility of curcumin, *Food Research International*, 2019, **125**, 108602.

7. Z. Wei, P. Zhu and Q. Huang, Investigation of ovotransferrin conformation and its complexation with sugar beet pectin, *Food Hydrocolloids*, 2019, **87**, 448–458.

8. Z. Wei and Q. Huang, Edible Pickering emulsions stabilized by ovotransferrin–gum arabic particles, *Food Hydrocolloids*, 2019, **89**, 590–601.

9. Z. Wei and Q. Huang, Assembly of protein–polysaccharide complexes for delivery of bioactive ingredients: A perspective paper, *J. Agric. Food Chem.*, 2019, **67**, 1344–1352.

10. O. G. Jones, S. Handschin, J. Adamcik, L. Harnau, S. Bolisetty and R. Mezzenga,

Complexation of β-lactoglobulin fibrils and sulfated polysaccharides, *Biomacromolecules*, 2011, **12**, 3056–3065.

11. Z. Gao, Y. Huang, B. Hu, K. Zhang, X. Xu, Y. Fang, K. Nishinari, G. O. Phillips and J. Yang, Interfacial and emulsifying properties of the electrostatic complex of β-lactoglobulin fibril and gum Arabic (*Acacia Seyal*), *Colloids Surf., A*, 2019, **562**, 1–7.

12. P. Gupta, K. Vermani and S. Garg, Hydrogels: from controlled release to pH-responsive drug delivery, *Drug Discovery Today*, 2002, **7**, 569–579.

13. S. I. Laneuville, S. L. Turgeon, C. Sanchez and P. Paquin, Gelation of native β-lactoglobulin induced by electrostatic attractive interaction with xanthan gum, *Langmuir*, 2006, **22**, 7351–7357.

14. X. T. Le, L. E. Rioux and S. L. Turgeon, Formation and functional properties of protein–polysaccharide electrostatic hydrogels in comparison to protein or polysaccharide hydrogels, *Adv. Colloid Interface Sci.*, 2017, **239**, 127–135.

15. R. Huang, W. Qi, L. Feng, R. Su and Z. He, Self-assembling peptide–polysaccharide hybrid hydrogel as a potential carrier for drug delivery, *Soft Matter*, 2011, **7**, 6222–6230.

16. W. Wijaya, P. Van der Meeren and A. R. Patel, Cold-set gelation of whey protein isolate and low-methoxyl pectin at low pH, *Food Hydrocolloids*, 2017, **65**, 35–45.

17. C. S. Wang, G. Natale, N. Virgilio and M. C. Heuzey, Synergistic gelation of gelatin B with xanthan gum, *Food Hydrocolloids*, 2016, **60**, 374–383.

18. X. T. Le and S. L. Turgeon, Rheological and structural study of electrostatic cross-linked xanthan gum hydrogels induced by β-lactoglobulin, *Soft Matter*, 2013, **9**, 3063–3073.

19. J. Adamcik, A. Berquand and R. Mezzenga, Single-step direct measurement of amyloid fibrils stiffness by peak force quantitative nanomechanical atomic force microscopy, *Appl. Phys. Lett.*, 2011, **98**, 193701.

20. Z. Wei and Q. Huang, In vitro digestion and stability under environmental stresses of ovotransferrin nanofibrils, *Food Hydrocolloids*, 2020, **99**, 105343.

21. Z. Wei and Q. Huang, Impact of covalent or non-covalent bound epigallocatechin-3-gallate (EGCG) on assembly, physicochemical characteristics and digestion of ovotransferrin fibrils, *Food Hydrocolloids*, 2020, **98**, 105314.

22. Z. Wei and Q. Huang, Ovotransferrin nanofibril formation in the presence of glycerol or sorbitol, *Food Chem.*, 2020, **305**, 125453.

23. Z. Wei and Q. Huang, Modulation of formation, physicochemical properties, and digestion of ovotransferrin nanofibrils with covalent or non-covalent bound gallic acid, *J. Agric. Food Chem.*, 2019, **67**, 9907–9915.

24. B. Katzbauer. Properties and applications of xanthan gum, *Appl. Phys. Lett.*, 1998, **59**, 81–84.

25. A. Maltais, G. E. Remondetto and M. Subirade, Soy protein cold-set hydrogels as controlled delivery devices for nutraceutical compounds, *Food Hydrocolloids*, 2009, **23**,

1647–1653.

26. H. S. Koop, R. A. de Freitas, M. M. de Souza, R. Savi-Jr and J. L. M. Silveira, Topical curcumin-loaded hydrogels obtained using galactomannan from *Schizolobium parahybae* and xanthan, *Carbohydr. Polym.*, 2015, **116**, 229–236.

27. J. Zhang, Y. Chen, H. Luo, L. Sun, M. Xu, J. Yu, Q. Zhou, G. Meng and S. Yang, Recent update on the pharmacological effects and mechanisms of dihydromyricetin, *Front. Pharmacol.*, 2018, **9**, 1204.

28. Z. Wei, Y. Cheng and Q. Huang, Heteroprotein complex formation of ovotransferrin and lysozyme: Fabrication of food-grade particles to stabilize Pickering emulsions, *Food Hydrocolloids*, 2019, **96**, 190–200.

29. M. S. M. Wee, S. Nurhazwani, K. W. J. Tan, K. K. T. Goh, I. M. Sims and L. Matia-Merino, Complex coacervation of an arabinogalactan-protein extracted from the *Meryta sinclarii* tree (puka gum) and whey protein isolate, *Food Hydrocolloids*, 2014, **42**, 130–138.

30. S. Roshanghias and A. Madadlou, Functional and gel properties of whey protein nanofibrils as influenced by partial substitution with cellulose nanocrystal and alginate, *Int. Dairy J.*, 2018, **81**, 53–61.

31. Q. Ru, Y. Wang, J. Lee, Y. Ding and Q. Huang, Turbidity and rheological properties of bovine serum albumin/pectin coacervates: Effect of salt concentration and initial protein/polysaccharide ratio, *Carbohydr. Polym.*, 2012, **88**, 838–846.

32. L. Liu, Q. Zhao, T. Liu, Z. Long, J. Kong and M. Zhao, Sodium caseinate/xanthan gum interactions in aqueous solution: Effect on protein adsorption at the oil-water interface, *Food Hydrocolloids*, 2012, **27**, 339–346.

33. A. Abaee and A. Madadlou, Niosome-loaded cold-set whey protein hydrogels, *Food Chem.*, 2016, **196**, 106–113.

34. C. Yang, Y. Wang and L. Chen, Fabrication, characterization and controlled release properties of oat protein gels with percolating structure induced by cold gelation, *Food Hydrocolloids*, 2017, **62**, 21–34.

35. A. Totosaus, J. G. Montejano, J. A. Salazar and I. Guerrero, A review of physical and chemical protein-gel induction, *Int. J. Food Sci. Technol.*, 2002, **37**, 589–601.

36. G. Copetti, M. Grassi, R. Lapasin and S. Pricl, Synergistic gelation of xanthan gum with locust bean gum: a rheological investigation, *Glycoconjugate J.*, 1997, **14**, 951–961.

37. A. M. Castilla, M. Wallace, L. L. E. Mears, E. R. Draper, J. Doutch, S. Rogers and D. J. Adams, On the syneresis of an OPV functionalised dipeptide hydrogel, *Biomater. Sci.*, 2016, **12**, 7848–7854.

38. S. Boral, A. Saxena and H. B. Bohidar, Syneresis in agar hydrogels, *Int. J. Biol. Macromol.*, 2010, **46**, 232–236.

39. M. Mohammadian and A. Madadlou, Cold-set hydrogels made of whey protein nanofibrils with different divalent cations, *Int. J. Biol. Macromol.*, 2016, **89**, 499–506.

40. E. M. Ahmed, Hydrogel: Preparation, characterization, and applications: A review, *J.*

Adv. Res., 2015, **6**, 105–121.

41. Z. Wei, Y. Cheng, J. Zhu and Q. Huang, Genipin-crosslinked ovotransferrin particle-stabilized Pickering emulsions as delivery vehicles for hesperidin, *Food Hydrocolloids*, 2019, **94**, 561–573.

42. Z. Wei and Q. Huang, Development of high internal phase Pickering emulsions stabilised by ovotransferrin–gum arabic particles as curcumin delivery vehicles, *Int. J. Food Sci. Technol.*, https://doi.org/10.1111/ijfs.14340.

43. Z. Wei, H. Zhang and Q. Huang, Curcumin-loaded Pickering emulsion stabilized by insoluble complexes involving ovotransferrin–gallic acid conjugates and carboxymethyldextran, *Food Funct.*, 2019, **10**, 4911–4923.

44. M. Lassé, D. Ulluwishewa, J. Healy, D. Thompson, A. Miller, N. Roy, K. Chitcholtan and J. A. Gerrard, Evaluation of protease resistance and toxicity of amyloid-like food fibrils from whey, soy, kidney bean, and egg white, *Food Chem.*, 2016, **192**, 491–498.

45. D. Kee, Q. Liu and J. Hinestroza, Viscoelastic (non-Fickian) diffusion, *Can. J. Chem. Eng.*, 2005, **83**, 913–929.

46. J. A. Ferreira, M. Grassi, E. Gudino and P. de Oliveira, A new look to non-Fickian diffusion, *Appl. Math. Modelling*, 2015, **39**, 194–204.

Figure captions:

Fig. 1. Turbidity as function of pH for OVT fibril, XG and OVT fibril–XG mixture (mass ratio $r = 2{:}1$).

Fig. 2. Zeta potential of OVT fibril, XG and OVT fibril–XG mixture (mass ratio $r = 2{:}1$).

Fig. 3. Photograph of OVT fibril dispersion (30 mg/mL) after inverting the vial for 10 s.

Fig. 4. (a) Photograph of XG solution (10 mg/mL) after inverting the vial for 24 h. (b) Photograph of XG hydrogel (30 mg/mL) after inverting the vial for 24 h.

Fig. 5. Visual appearance of hydrogel assembled from OVT fibril and XG at pH 4.0: (a) non-inverted vial, (b) inverted vial after 24 h-storage. The pH was adjusted with addition of glucono delta-lactone (GDL).

Fig. 6. Visual appearance of hydrogel assembled from OVT fibril and XG at pH 4.0. The pH was adjusted with addition of HCl.

Fig. 7. (a) SEM image of XG gel. (b) SEM image of OVT fibril–XG gel.

Fig. 8. (a) Storage modulus (G′) and loss modulus (G″) of XG gel and OVT fibril–XG gel as function of oscillatory frequency. (b) Apparent viscosity of XG gel and OVT fibril–XG gel as function of shear rate.

Fig. 9. (a) DMY dispersion (1 mg/mL) without heating treatment or storage. (b) DMY solution (2 mg/mL) after heating at 60 °C for 5 min. (c) Heated DMY solution (2 mg/mL) after storage at 25 °C for 6 h.

Fig. 10. Release profile of DMY from XG gel and OVT fibril–XG gel.
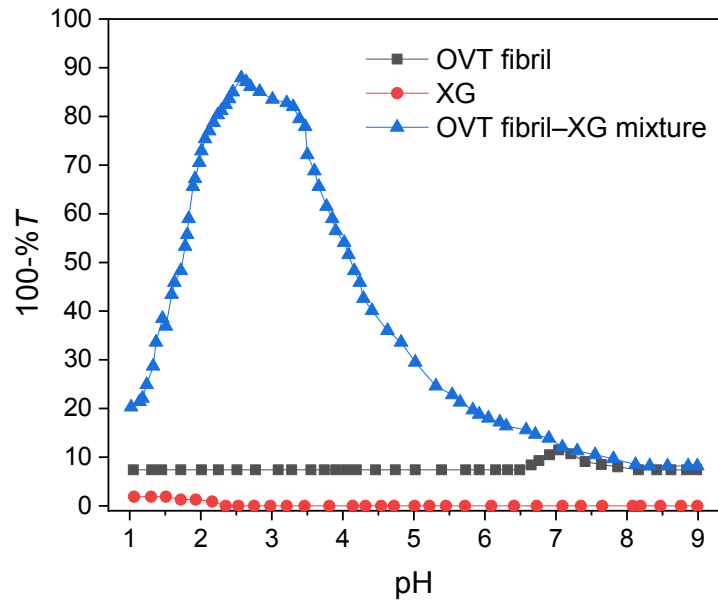
Fig. 1
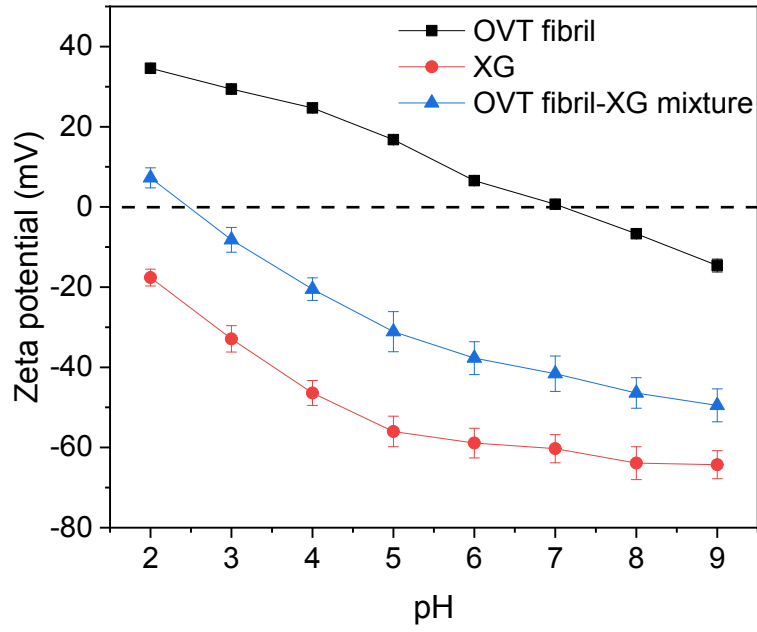
Fig. 2

Fig. 3

(a)   (b)
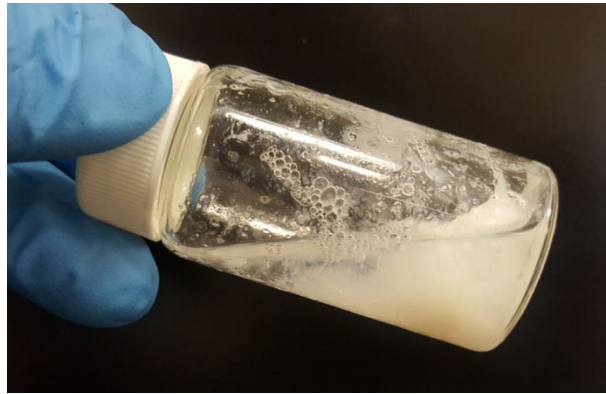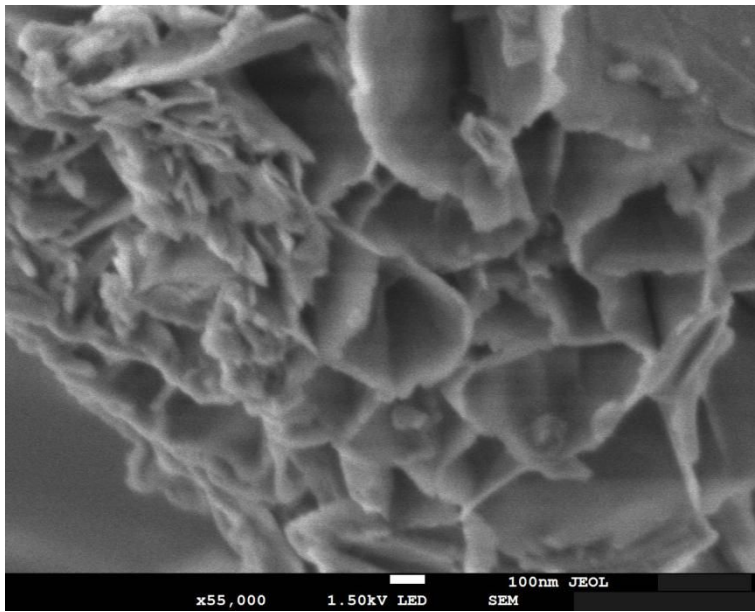
Fig. 4

(a)   (b)
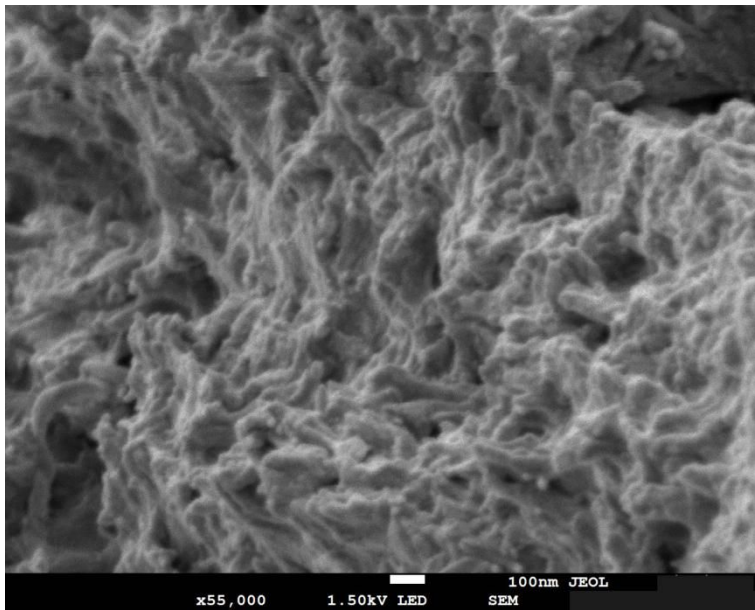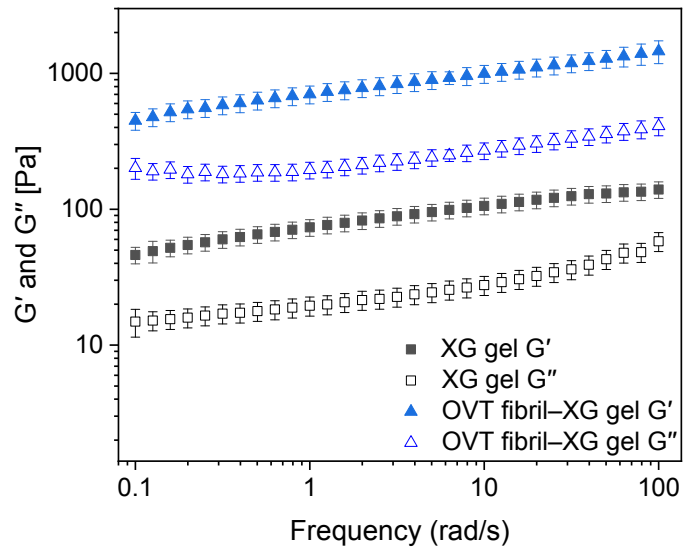
Fig. 5

Fig. 6

(a)

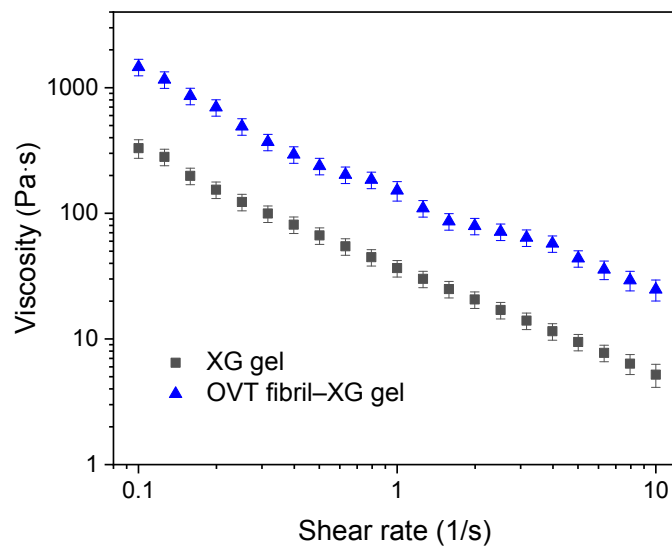

(b)

Fig. 7

(a)
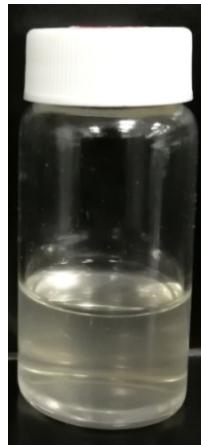

(b)
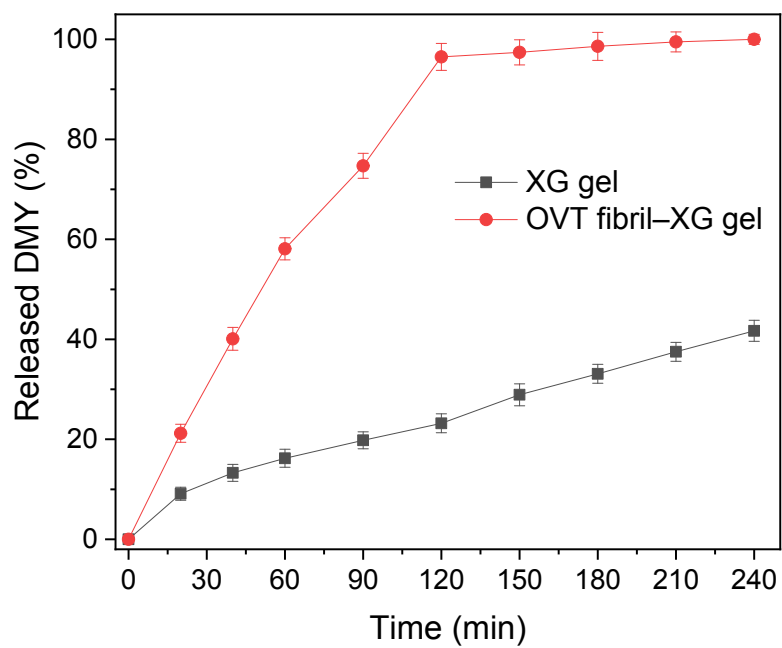
Fig. 8

(a)   (b)   (c)
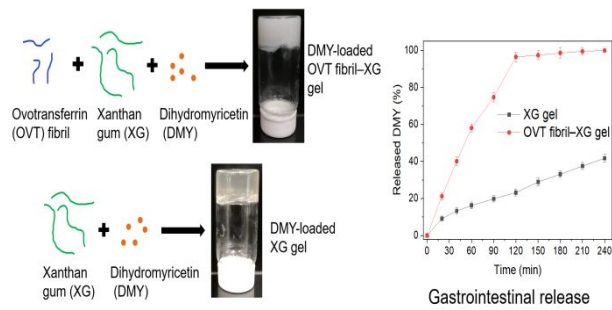
Fig. 9

Fig. 10

Table 1. Synerisis and water holding capacity of XG gel and OVT fibril–XG gel

Gel samples	Synerisis (%)	water holding capacity (%)
XG gel	0.0±0.0	100.0±0.0
OVT fibril–XG gel	0.0±0.0	95.8±0.5

Table of Contents

Novel ovotransferrin fibril–xanthan gum hydrogels were assembled to deliver dihydromyricetin effectively.